Supporting Information for:

Nanoparticles for inhibition of *in vitro* tumour angiogenesis: synergistic actions of ligand function and laser irradiation

Dorota Bartczak, [a,b] Otto L. Muskens, [a,c] Simone Nitti, [d] Timothy M. Millar[b] and Antonios G. Kanaras[*,a,c]

[a] Physics and Astronomy, Faculty of Applied and Physical Sciences, University of Southampton, Southampton, SO17 1BJ, UK; [b] Faculty of Medicine, Southampton General Hospital, University of Southampton, Southampton, SO17 1BJ, UK; [c] Institute for Life Sciences, University of Southampton, Southampton, SO17 1BJ, UK; [d] Istituto Italiano di Technologia, Via Morego 30, 16163 Genova, Italy.

Table of contents:

S1. Physicochemical characterization of nanorods

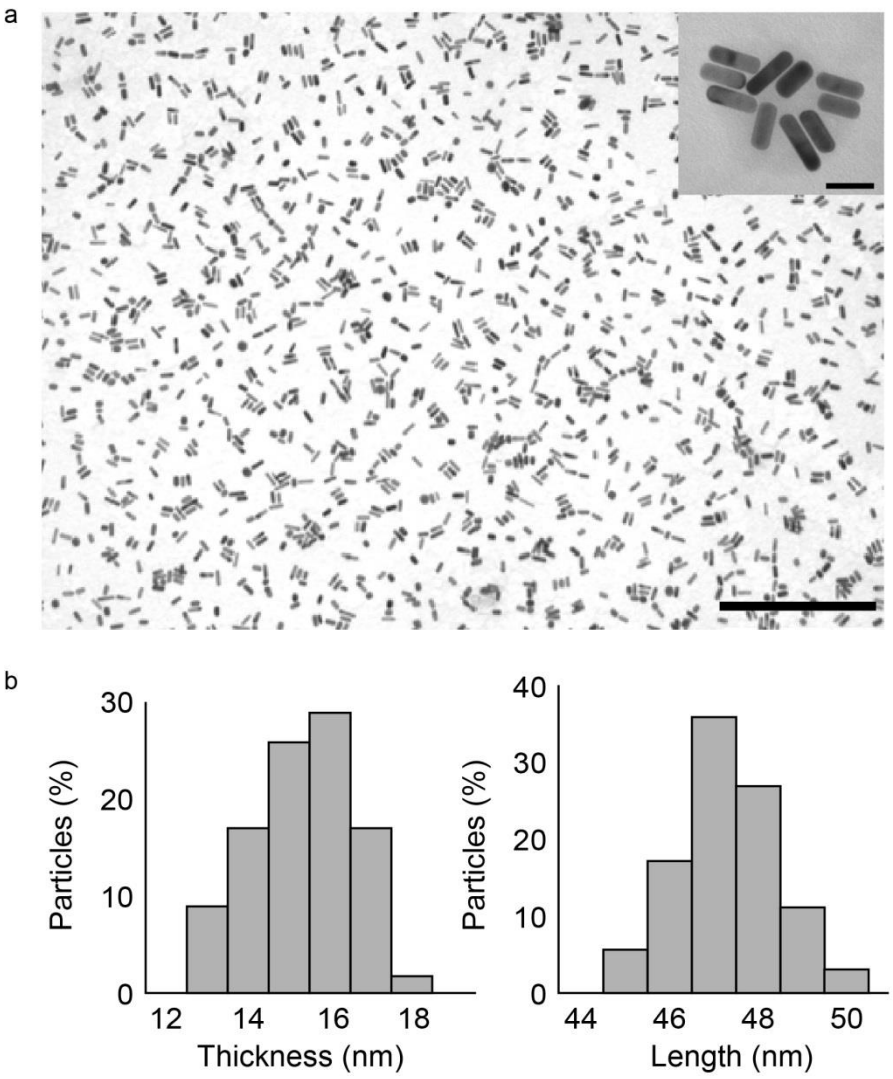

Figure S1A. a Transmission electron microscopy image of gold nanorods used in experiments. Scale bars 500nm (main image) and 50nm (inset). **b** Histograms show measured distributions for nanorod width and length.

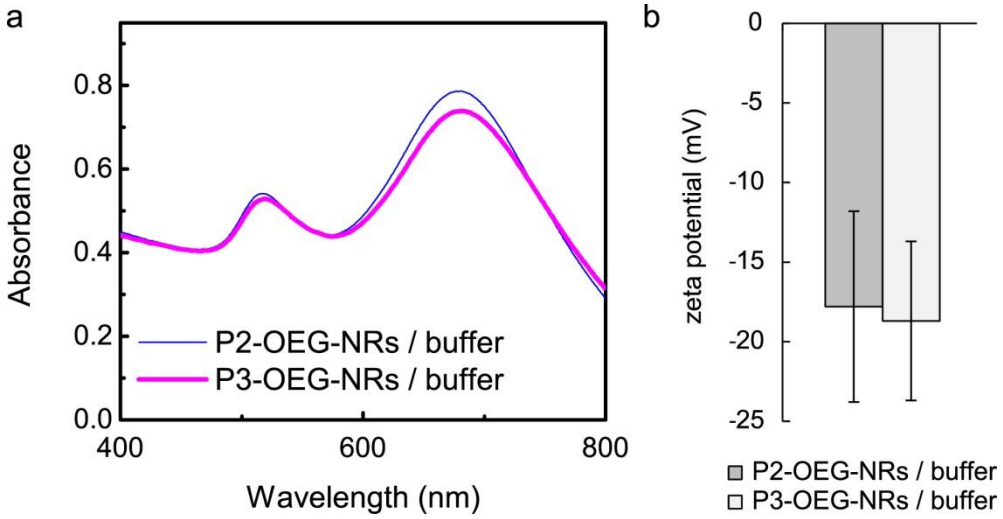

Figure S1B. UV-Vis spectra (**a**) and Zeta-potential (**b**) of P2-OEG-NRs and P3-OEG-NRs in sodium borate buffer.

Number of peptides covalently attached to gold nanorods.

The number of peptides per nanorod was estimated using FluoroProfile Protein Quantification Kit (Sigma-Aldrich). A 'working reagent' was prepared according to manufacturer recommendation by mixing the fluorescent reagent, quantification buffer and water in the ratio volume: 1:1:8. The 'working reagent' (50 µl) was added to the quantified solution (50 µl, supernatant left after nanorods purification) and shaken. The reaction mixture was incubated for 30 min. at room temperature in the dark. The maximum emission measured at 620 nm with 510 nm was used to calculate the number of peptides from a calibration curve, prepared with known quantities of the peptide. This number was then subtracted from the known concentration of peptide introduced into the NR solution, to give the quantity of peptide bound to NR. The concentration of gold in NR was estimated with inductively coupled plasma mass spectroscopy, whilst having calculated the average number of atoms per nanorod of known dimensions, the total number of NR in the sample was derived. The number (moles) of bound peptides was then divided by the number of NR in the sample, to give the number of peptides per nanorod. This was estimated to be 1364 ± 132 per nanorod.

S2. Processing of the nanoparticle/cell samples

Preparation of samples for transmission electron microscopy:

Confluent HUVEC, MDA-MB-231 and MCF-7 cell monolayer were exposed to P2-OEG-NRs and P3-OEG-NRs (3nM, in 20% HS M199 growth media for EC and 10% HS DMEM for cancer cells) for 4 h at 37 °C in a humidified 5 % CO_2 balanced air incubator. After treatment, cells were washed three times with PBS (1 x), then trypsinised (0.75 ml, 0.25 % trypsin 0.01 % EDTA solution, Sigma-Aldrich) for 5 min. at 37 °C in 5 % CO_2. The cell suspension was transferred to a plastic tube (1.5 ml, Eppendorf) and centrifuged (2500 rpm, 5 min, 4 °C). The solution was decanted and the cell pellet was redispersed in a main fixative: glutaraldehyde / formaldehyde (3 % / 4 %, in 0.1 M piperazine-1,4-bis (2-ethanesulfonic acid - PIPES buffer, pH 7.2), then incubated for 15 min. at room temperature. Cells were centrifuged (2500 rpm, 5 min, 4 °C) and decanted. To the cell pellet a drop of sodium alginate (5 % in water) was introduced with a mixture of PIPES buffer (0.5 ml, 0.2 M) and calcium chloride solution (0.5 ml, 0.2 M in water). When the alginate settled (15 min.), the supernatant was removed and the embedded cell pellet was transferred into a glass vial and fixed with post fixative: osmium tetroxide (1 %, 0.1 M PIPES buffer) for 1 h. The fixed pellet was washed twice with water (for 5 min.) and stained with uranyl acetate (2 %, in water) for 20 min. The specimen was washed with 30 %, 50 %, 70 % and 95 % ethanolic solutions for 10 min. each, then absolute ethanol for 20 min. twice. Dehydrated cells were embedded in TAAB resin (Agar Scientific Ltd.) and polymerised at 60 °C for 24 h. Resin blocks were cut using Leica RM 2255 microtome to obtain ultrathin sections (~ 90 nm thickness). Sections were deposited on TEM grids and stained with Reynolds lead stain prior to imaging.

Preparation of samples for ICP-OES:

HUVEC, MDA-MB-231 and MCF-7 cells (100 000/well) grown on porcine gelatin (0.2 % in HBSS) pre-coated 12-well micro-plate were incubated with P1-NR and P3-NR (3nM, in 20% HS M199 growth media for EC and 10% HS DMEM for cancer cells) for 4 h at 37 °C in a humidified 5 % CO_2 balanced air incubator. After treatment, cells were washed three times with PBS (1 x), trypsinised (0.75 ml, 0.25 % trypsin 0.01 % EDTA solution, Sigma-Aldrich) and the cell suspension was transferred into a plastic tube (15 ml) and centrifuged (2'500 rpm, 5 min., 4 °C). The cell pellet was redispersed in PBS (1 ml, 1 x), counted and transferred into a glass vial. Cells where then digested with aqua regia (9 ml) and a series of dilution was measured using gold standards.

The amount of gold atoms in each sample was measured in ppm, while the number of cells was counted. This was referred to the total amount of introduced NPs and the background level of gold in cells, both measured by ICP-OES. The number of gold atoms per nanoparticle was 'roughly' estimated from the average size of NPs (measured by TEM), the distances between atoms in the fcc crystal structure and the volume of a gold atom. The average number of NPs per cell was then calculated. At least three independent experiments were performed to estimate average numbers.

S3. Cell sensitivity to laser light.

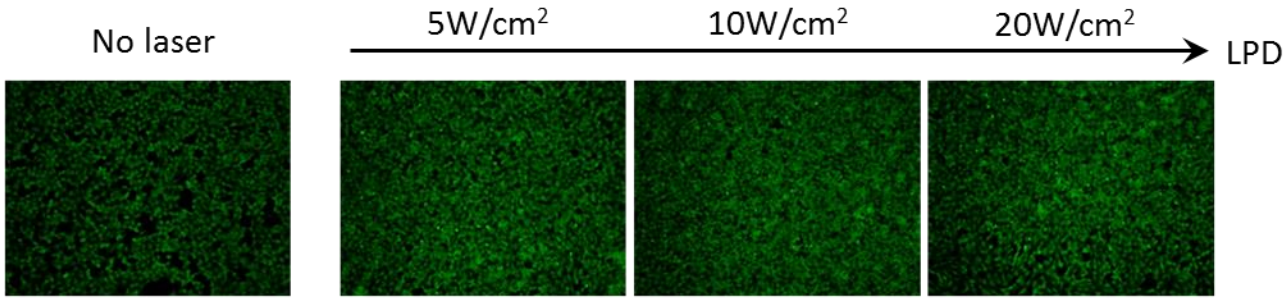

Figure S3. Fluorescent images (Calcein Green) of HUVEC monolayer exposed to increasing laser power, demonstrating that the LPD range used, does not ablate cells or affect their availability.

S4. Fluorescent images and quantification of capillaries stimulated with MCF-7 conditioned media and treated with various doses of peptide coated gold nanorods and laser irradiation.

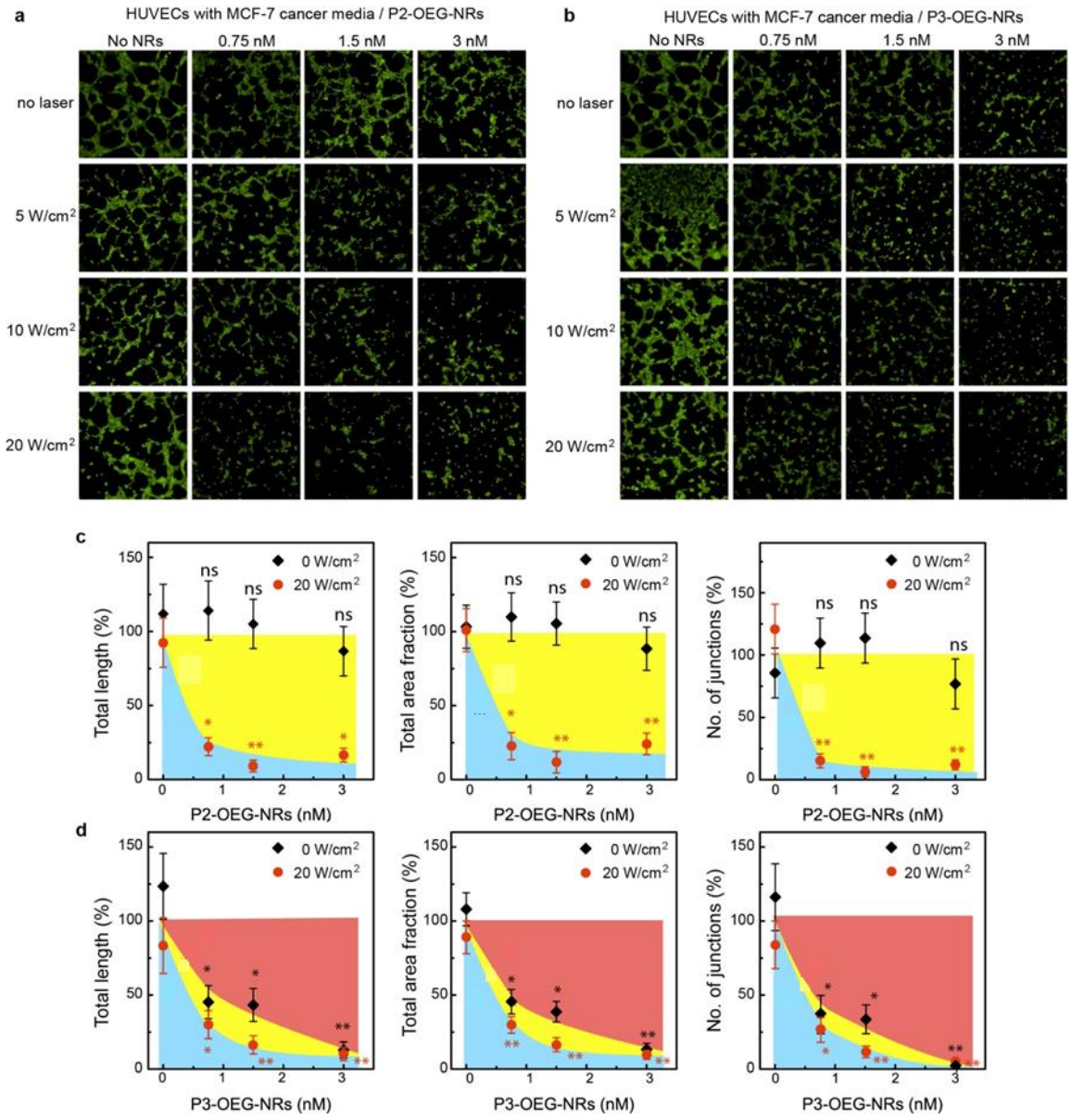

Figure S4. Inhibition of angiogenesis stimulated with MCF-7 cancer cell conditioned media. Fluorescent images and quantification of capillaries stimulated with MCF-7 conditioned media and treated with various doses of P2-OEG-NRs (a) or P3-OEG-NRs (b) and laser irradiation. In (c, d) a quantitative analysis of the vascular network is shown; tubule length, fraction area and number of junctions; n=3, average ± stdev; *p≤0.05, **p≤0.01. Coloured regions indicate anti-angiogenic biological activity in the vascular network (red), additional effect of laser irradiation (yellow), and unaffected network (blue).

S5. Fluorescent images and quantification of capillaries stimulated with MCF-7 cancer cells and treated with various doses of peptide coated gold nanorods and laser irradiation.

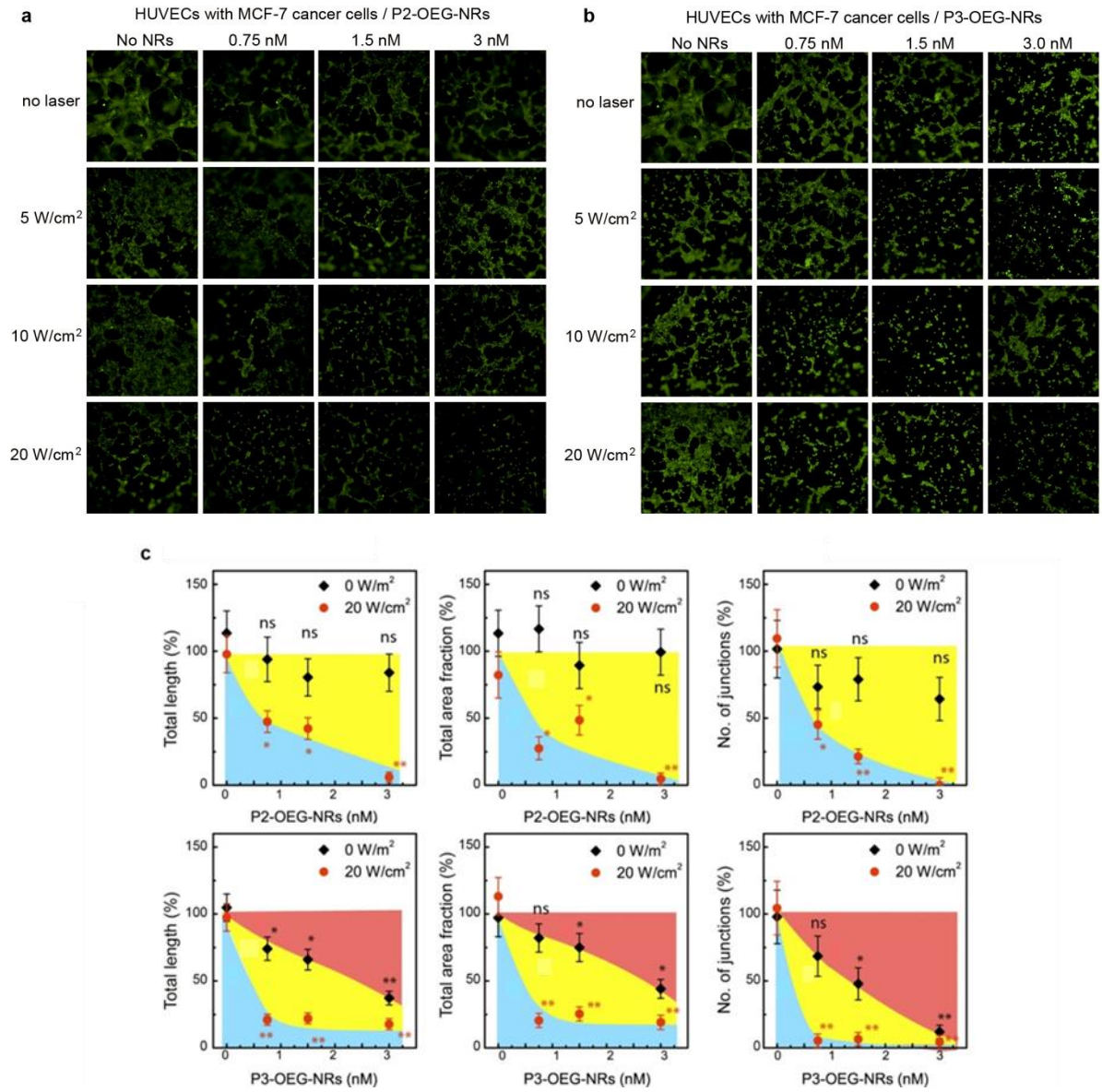

Figure S5. Inhibition of angiogenesis stimulated with co-cultured MCF-7 cancer cells. Fluorescent images and quantification of capillaries stimulated from MCF-7 cancer cells and treated with various doses of P2-OEG-GNRs (a) or P3-OEG-NRs (b) and laser irradiation. In (c) a quantitative analysis of the vascular network is shown; tubule length, fraction area and number of junctions; n=3, average ± stdev; *p≤0.05, **p≤0.01. Colored regions indicate anti-angiogenic biological activity in the vascular network (red), additional effect of laser irradiation (yellow), and unaffected network (blue).

S6. Fluorescent images of capillaries stimulated with MDA-MB-231 cancer cells and treated with various doses of peptide coated gold nanorods and laser irradiation.

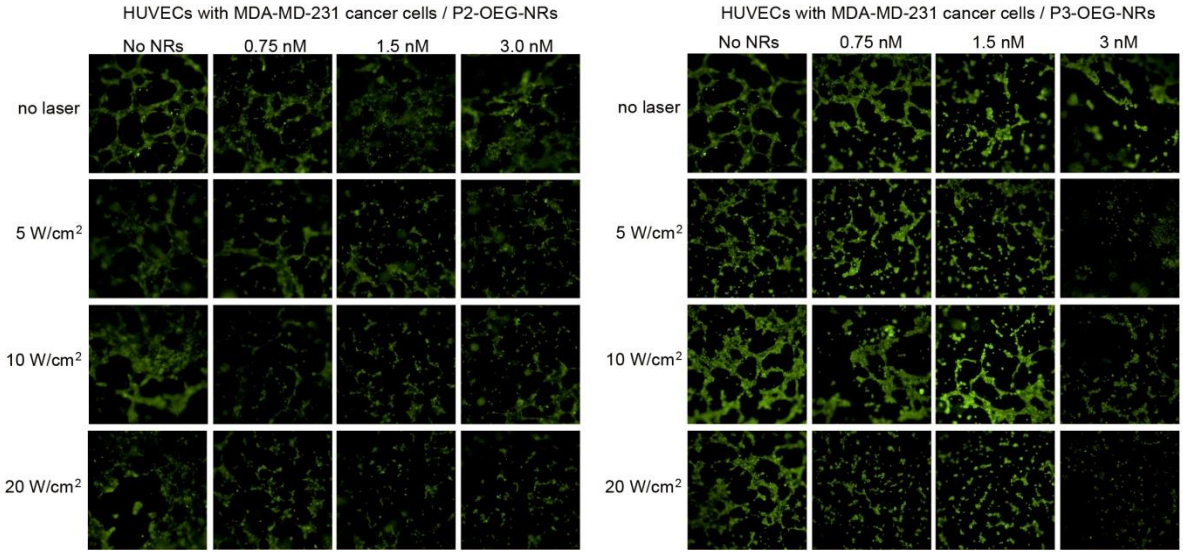

Figure S6. A full range of fluorescent images of capillaries stimulated from MDA-MB-231 cancer cells and treated with various doses of peptide coated gold nanorods and laser irradiation.

S7. Full quantification of capillaries stimulated with MDA-MB-231 conditioned media or MDA-MB-231 co-cultured cells and treated with various doses of peptide coated gold nanorods and laser irradiation.

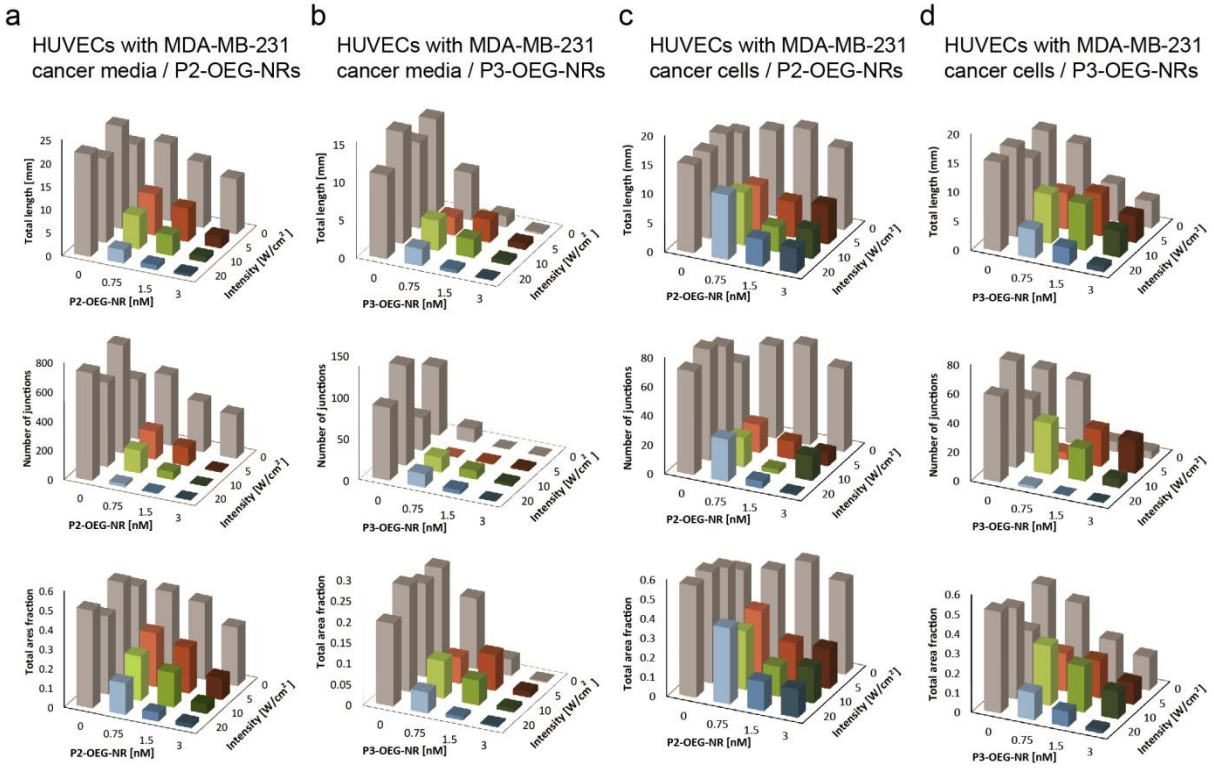

Figure S7. Full statistical analysis of tubule length, area fraction and number of junctions for all combinations of peptide-coated gold nanorod dose and laser irradiation.

S8. Full quantification of capillaries stimulated with MCF-7 conditioned media or co-cultured MCF-7 cells and treated with various doses of peptide coated gold nanorods and laser irradiation.

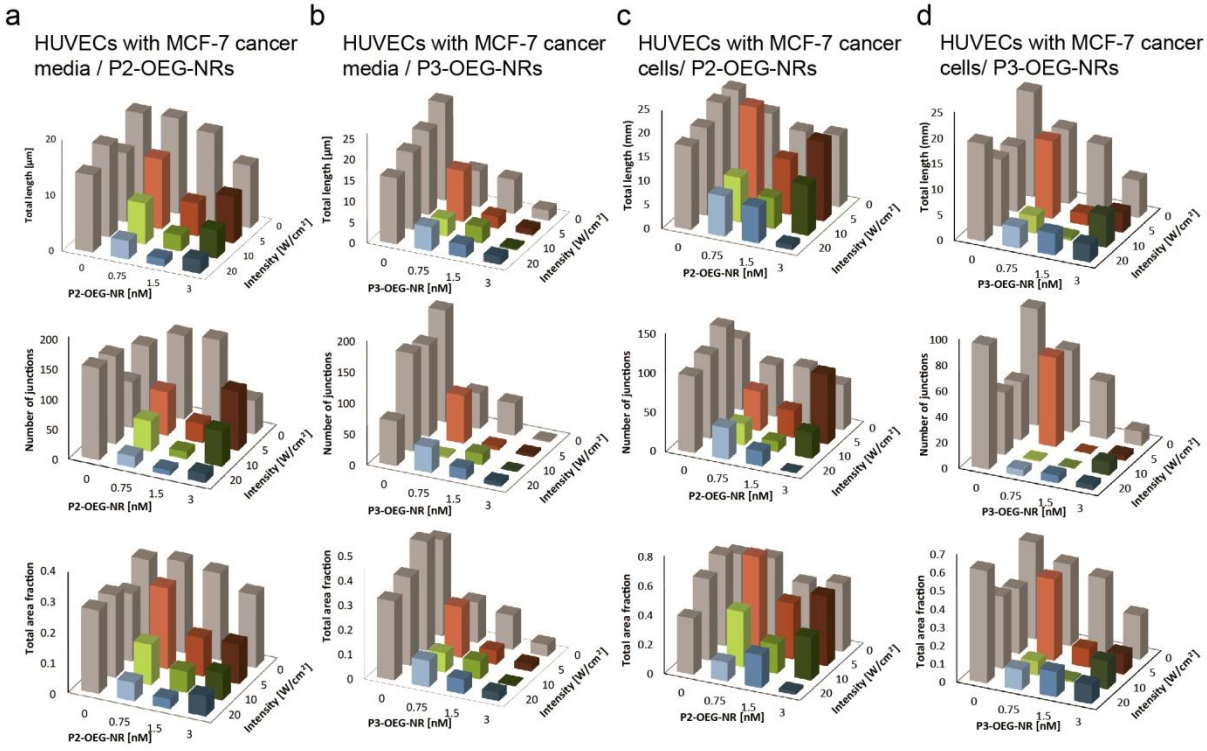

Figure S8. Full statistical analysis of tubule length, area fraction and number of junctions for all combinations of peptide-coated gold nanorod dose and laser irradiation.

S9. Peptide coated nanorods binding to cell receptors.

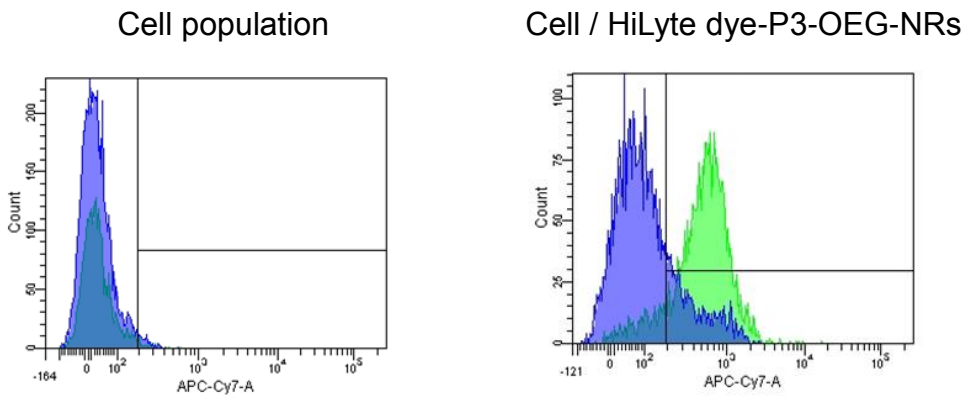

Figure S9. Peptide coated gold nanorods binding to HUVECs, as determined by flow cytometry. Control shows cells only. Cells exposed to fluorescent dye labelled rods (HiLyte 680-P3-OEG-NRs) show fluorescence (binding). Note: the flow cytometry assay, as well as the nanoparticles labelling with a fluorophore was performed according to a protocol described before.[1]

S10. Explanation of Angioquant image analysis and extraction of angiogenesis parameters total area fraction, total network length and number of nodes.

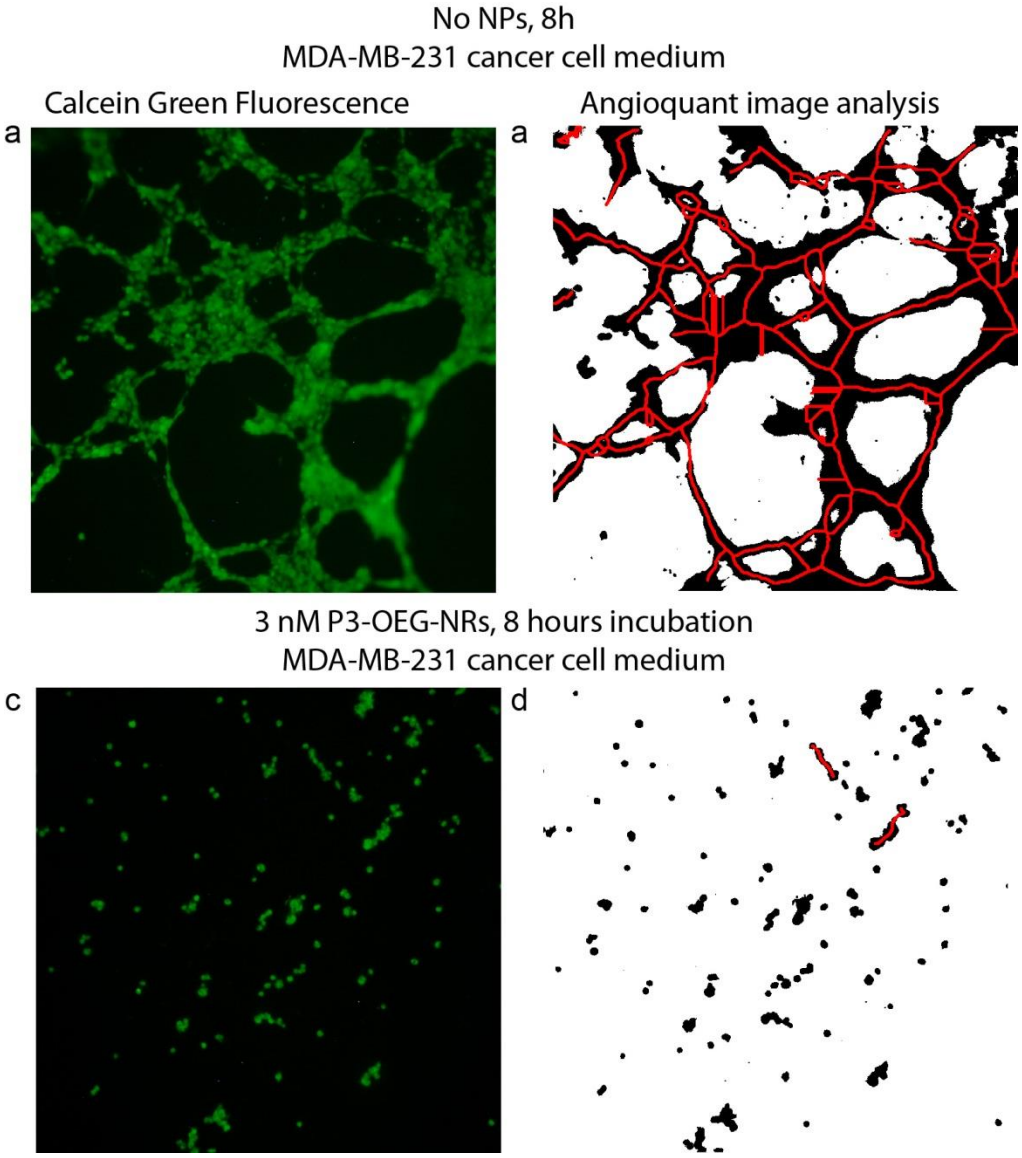

Figure S10. Example of image analysis using Angioquant software using typical images taken 8 hours after incubation, for the condition without nanoparticles and laser (a,b), and in presence of 3 nM P3-OEG-NRs (c,d). Calcein green fluorescence images were converted to grayscale, inverted and thresholded to obtain a binary image where the cellular network is indicated by black areas. The total area fraction was obtained from this binary image. Subsequently, the algorithm of Ref. 2 was used to thin down the network to a single pixel skeleton. Segments of the skeleton shorter than the typical size of a single cell were pruned from the skeleton using a 100 pixel cutoff length. From the pruned skeleton, as indicated by the red lines in b and d, the total length and number of nodes were obtained.

References:

1. Bartczak D., Sanchez-Elsner T., Louafi F., Millar T., Kanaras, A. G. Receptor-mediated interactions between colloidal gold nanoparticles and human umbilical vein endothelial cells. *Small* **7,** 388–394 (2011).
2. Niemistö, A., Dunmire, V., Yli-Harja, O., Zhang, W., Shmulevich, I. Robust quantification of in vitro angiogenesis through image analysis. IEEE Transactions on Medical Imaging 24, 549-553 (2005).